

Global Minimum Torque Ripple Design for Direct Torque Control of Induction Motor Drives

Kuo-Kai Shyu, *Member, IEEE*, Juu-Kuh Lin, Van-Truong Pham, Ming-Ji Yang, and Te-Wei Wang

Abstract—This paper proposes a simple but effective method to reduce the torque ripple for direct torque control (DTC) of induction motor drives. The proposed DTC provides a global minimum torque ripple, which satisfies the root-mean-square (rms) criteria of torque ripple. Such a global minimum torque ripple DTC has not been derived before. The proposed global minimum torque ripple DTC is a two-step design. The first step drives the torque error to zero at the end of the control period. Then, the second step reduces the torque bias and rms ripple by modifying the asymmetry switching patterns of the applied voltage vectors of the first step into symmetry ones. Theoretical analysis is provided to show that the torque ripple of the proposed DTC is a global minimum rms ripple. Furthermore, to verify the effectiveness of this study, a DSP-based experimental induction motor DTC drive system is built. Simulation and experimental results verify that the torque ripple performance has been improved.

Index Terms—Induction motor drives, minimization methods, pulsewidth-modulated inverters, torque control.

I. INTRODUCTION

THE DESIGN of a high-performance induction motor drive, one of the most significant developments is the field-oriented control (FOC), in which the essential work is to identify the spatial position of the rotor flux and stator current. In this way, the electromagnetic torque is fundamentally the cross product of the flux and current in the same manner as a dc motor [1], [2], [21], [22]. However, for FOC, the flux angle is needed for transformation, which is sensitive to identification method. Another method uses the nonlinear control theory, such as a feedback linearization controller, to achieve input–output decoupling [3], [4], [23]–[26]. Nonlinear control using nonlinear feedback linearization does not require a computation of this angle. However, it is complicated in the algorithm.

Direct torque control (DTC) has been recognized in recent decades as a viable control method for high-performance motor drivers [5]–[20] since it was invented by Takahashi and

Noguchi [5] and Depenbrock [6] (as direct self-control). In addition, it minimizes the use of machine parameters and reduces the complexity of the algorithms involved in FOC and feedback linearization methods. Note that FOC tries to reproduce the high dynamic behavior of a dc motor. The torque could be expressed by the product of the rotor flux and the stator current. It has to produce the rotor flux and the stator current. It has to know the phase angle of the rotor flux vector. As a result, FOC is achieved by controlling the direct and quadrature stator currents onto the desired ones. However, different from FOC, DTC does not try to reproduce the dynamical behavior of a dc motor but is aimed at the flux- and torque-producing capabilities of an induction motor fed by an inverter. Another expression of the torque, different from the torque expression used in FOC, could be the product of the rotor flux and stator flux. It is noticed that the stator flux can be directly adjusted by the stator voltage. Accordingly, DTC has advantages of high torque response and simple realization. Therefore, flux- and torque-producing capabilities could be achieved. However, two major drawbacks of DTC are normally addressed [10], [13], [16], [18], [20]. One is that the switching frequency varies according to the motor speed and the hysteresis bands of torque and flux. Another is that a high torque ripple is generated.

To solve the aforementioned problems of varying switching frequency and torque ripple, a commonly used way is the space vector modulation (SVM). The concept of SVM was first proposed by Habetler *et al.* [7]. They calculate the inverter switching pattern or duty cycle directly in order to control the torque and flux over a constant switching period. Later, by using the concept of SVM, many approaches of DTC-controlled induction motor drives have been developed [8]–[20].

The common concept to reducing the torque ripple is the synthesis of a higher number of voltage space vectors with respect to those used in basic DTC techniques. That means each switching period is subdivided into three or more states to synthesize the voltage vectors in order to generate minimum torque ripple. From theoretical point of view, the minimization problem is supposed to first define a criterion related to the minimization object. Then, the problem is solved by minimizing the criterion. However, those studies, without minimizing any kind of torque ripple performance criterion, presented voltage switching patterns to reduce the torque ripple by introducing control methods.

Among those DTC studies on reducing torque ripples, only few of them proposed voltage switching patterns by minimizing the root-mean-square (rms) torque ripple performance criteria while maintaining a constant switching frequency [10], [13], [20]. By minimizing the rms torque ripple performance index,

Manuscript received February 4, 2009; revised May 11, 2009 and August 24, 2009; accepted October 5, 2009. Date of publication December 31, 2009; date of current version August 11, 2010. This work was supported in part by the National Science Council of Taiwan under Contract NSC 96-2221-E-008-121-MY3.

K.-K. Shyu, J.-K. Lin, V.-T. Pham, and T.-W. Wang are with the Department of Electrical Engineering, National Central University, Chung-Li 32001, Taiwan (e-mail: kkshyu@ee.ncu.edu.tw; shine32@ms63.hinet.net; 965401601@cc.ncu.edu.tw; 945201086@cc.ncu.edu.tw).

M.-J. Yang was with the Department of Electrical Engineering, National Central University, Chung-Li 32001, Taiwan. He is now with Inskay Energy Technology Co., Chung-Li 32001, Taiwan (e-mail: s9521089@cc.ncu.edu.tw).

Color versions of one or more of the figures in this paper are available online at <http://ieeexplore.ieee.org>.

Digital Object Identifier 10.1109/TIE.2009.2038401

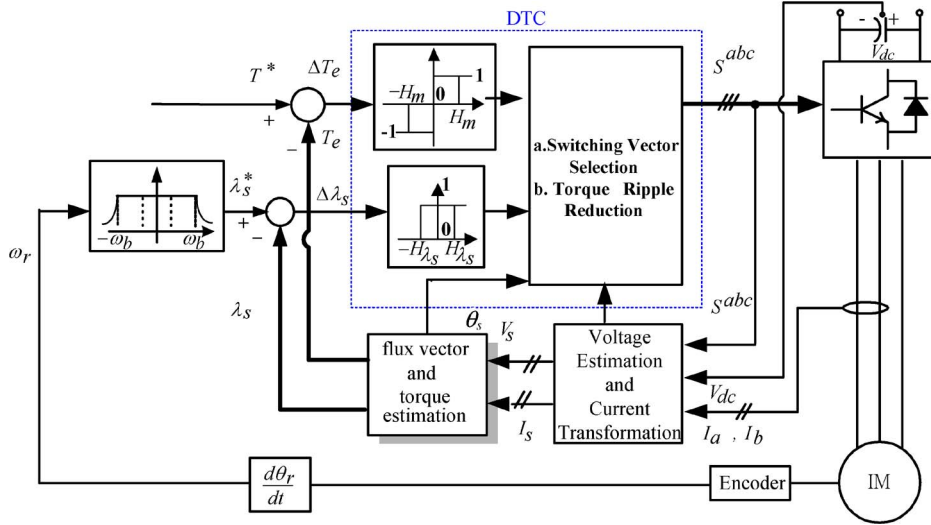


Fig. 1. Block diagram of DTC of an induction motor.

Kang and Sul [10] and Lee and Song [13] presented a three-level torque ripple reduction DTC. Abad *et al.* [20] proposed a two-level one. They proposed an analytical study about predicting the evolution of the torque and flux as a function of the applied voltage vector and mechanical speed. They, using the conventional DTC switching table, determine the pulse duration of the applied voltage vector by minimizing the rms torque ripple equation during one switching period. However, it should be noted that the rms torque ripple among those studies is a function of the starting torque error of every switching interval. However, the starting torque error varies for every switching interval. This means that to achieve the global rms minimum torque ripple is impossible. As a result, this paper, based on the same switching table, presents a new DTC having properties not only of constant switching frequency but also of the global minimum rms torque ripple.

The proposed DTC is a two-step design. The first step designs a nonzero voltage vector followed by a zero one to drive the torque error to zero at the end of the control period. Once the torque error at the end of the control period is driven to zero, the following control period starts with zero torque error. Directly applying a nonzero voltage vector followed by a zero voltage vector could cause torque bias and large rms ripple. Then, the second step design is to reduce the torque bias and rms ripple. The voltage vectors designed in the first step are modified in a symmetry switching pattern while maintaining zero torques at the beginning and the end of the control period as derived in the first step. This modification not only deletes the torque bias but also reduces the rms torque ripple.

Moreover, following the proposed two-step design, this study provides theoretical analysis that proves that the rms torque ripple is global minimum, which has not been done before.

Finally, simulation results are first provided to verify the effectiveness of the proposed method. Moreover, to verify the feasibility of this study, a fixed-point TMS320F240 DSP-based hardware experimental system is built to demonstrate the effectiveness of the proposed method. Experimental results show that the torque ripple is effectively reduced while comparing with the torque ripple minimization control method in [10].

 TABLE I
SWITCHING LOOKUP TABLE

λ_s in sector k	Torque (ΔT_e)		
	\uparrow	\downarrow	
Flux ($\Delta \lambda_s$)	\uparrow	V_{k+1}	V_0, V_7
	\downarrow	V_{k+2}	V_0, V_7

The organization of this paper is as follows. The proposed torque controller is presented in Section II. Some simulation and experimental results are given in Section III. Finally, Section IV gives the conclusions to this paper.

II. GLOBAL MINIMUM RMS TORQUE RIPPLE STRATEGY

First, the block diagram of the DTC induction motor drive is shown in Fig. 1, in which the applied voltage is based on the switching table given as Table I. Before presenting the proposed torque ripple reduction method with global minimum rms property, the previous related minimum rms torque reduction one is briefly introduced.

A. Minimum RMS Torque Ripple Method

The state-variable form of induction motor equations with stator and rotor flux vectors as state variables can be expressed by the following equation [10]:

$$\begin{bmatrix} \frac{d\lambda_s}{dt} \\ \frac{d\lambda_r}{dt} \end{bmatrix} = \begin{bmatrix} \frac{-R_s}{\sigma L_s} & \frac{R_s L_m}{\sigma L_s L_r} \\ \frac{R_r L_m}{\sigma L_s L_r} & j\omega_r - \frac{R_r}{\sigma L_r} \end{bmatrix} \begin{bmatrix} \lambda_s \\ \lambda_r \end{bmatrix} + \begin{bmatrix} 1 \\ 0 \end{bmatrix} V_s \quad (1)$$

and the electromagnetic torque is expressed in terms of the stator and rotor fluxes as

$$T = \left(\frac{3}{2}\right) \left(\frac{P}{2}\right) \frac{L_m}{\sigma L_s L_r} \text{Im}[\lambda_s \cdot \lambda_r^*] \quad (2)$$

where R_s is the stator resistance, R_r is the rotor resistance, V_s is the nonzero voltage vector, L_s and L_r are the stator and rotor inductances, L_m is the mutual inductance, and “*” denotes the complex conjugate.

For a small control period t_{sp} , stator and rotor fluxes at $(k + 1)$ th sampling instant can be written as

$$\lambda_{sK+1} = \lambda_{sK} + \left(\frac{-R_s}{\sigma L_s} \lambda_{sK} + \frac{R_s L_m}{\sigma L_s L_r} \lambda_{rK} + V_k \right) t_{sp} \quad (3)$$

$$\lambda_{rK+1} = \lambda_{rK} + \left(\frac{R_r L_m}{\sigma L_s L_r} \lambda_{sK} + \left(j\omega_r - \frac{R_r}{\sigma L_r} \right) \lambda_{rK} \right) t_{sp} \quad (4)$$

where $\lambda_{s(r)K}$ and $\lambda_{s(r)K+1}$ are the stator (rotor) fluxes at k th and $(k + 1)$ th sampling instants, respectively. V_k is a nonzero voltage vector.

By substituting (3) and (4) into the discrete form of (2), the torque increment by applying a nonzero voltage vector during one cycle time t_{sp} at the $(k + 1)$ th sampling instant can be expressed as

$$\begin{aligned} \Delta T_{eK+1} &= \left\{ -T_{eK} \left(\frac{-R_s}{\sigma L_s} + \frac{R_{rm}}{\sigma L_r} \right) + \left(\frac{3}{2} \right) \left(\frac{P}{2} \right) \right. \\ &\quad \times \left. \frac{L_m}{\sigma L_s L_r} \text{Im} \{ [V_k \cdot \lambda_{rk}^*] - j\omega_r [\psi_{sk} \cdot \lambda_{rk}^*] \} \right\} t_{sp} \\ &= S_1 t_{sp} \end{aligned}$$

where

$$\begin{aligned} S_1 &= \left\{ -T_{eK} \left(\frac{-R_s}{\sigma L_s} + \frac{R_{rm}}{\sigma L_r} \right) + \left(\frac{3}{2} \right) \left(\frac{P}{2} \right) \right. \\ &\quad \times \left. \frac{L_m}{\sigma L_s L_r} \text{Im} \{ [V_k \cdot \lambda_{rk}^*] - j\omega_r [\lambda_{sk} \cdot \lambda_{rk}^*] \} \right\}. \quad (5) \end{aligned}$$

Similarly, the torque decrement by applying a zero voltage vector during one cycle time t_{sp} at the $(k + 1)$ th sampling instant is

$$\begin{aligned} \Delta T_{eK+1} &= \left\{ -T_{eK} \left(\frac{-R_s}{\sigma L_s} + \frac{R_{rm}}{\sigma L_r} \right) + \left(\frac{3}{2} \right) \left(\frac{P}{2} \right) \right. \\ &\quad \times \left. \frac{L_m}{\sigma L_s L_r} \text{Im} \{ -j\omega_r [\lambda_{sk} \cdot \lambda_{rk}^*] \} \right\} t_{sp} \\ &= S_0 t_{sp} \end{aligned}$$

where

$$\begin{aligned} S_0 &= \left\{ -T_{eK} \left(\frac{-R_s}{\sigma L_s} + \frac{R_{rm}}{\sigma L_r} \right) + \left(\frac{3}{2} \right) \left(\frac{P}{2} \right) \right. \\ &\quad \times \left. \frac{L_m}{\sigma L_s L_r} \text{Im} \{ -j\omega_r [\lambda_{sk} \cdot \lambda_{rk}^*] \} \right\}. \quad (6) \end{aligned}$$

For a small control period t_{sp} , all variables could be taken as invariant. Thus, slopes S_0 and S_1 are constants within the calculated interval. In each control period t_{sp} , a nonzero voltage vector V_k and a zero voltage vector V_0 are applied with time durations t_s and $(t_{sp} - t_s)$, respectively. Generally, to evaluate the performance of a signal that differs from its reference one, rms is a commonly used way. The rms is defined over the interested time interval. For example, here, one is to evaluate the torque ripple between the actual torque T and the reference

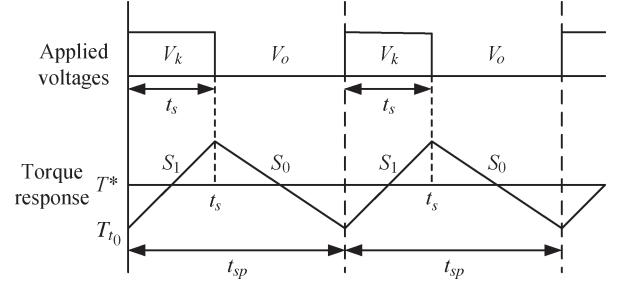


Fig. 2. Applied voltages and torque response of minimum ripple DTC [10].

torque T^* over a time period t_{sp} . One could first define the torque error as

$$T_{\text{error}} = T - T^*.$$

Then, the rms value of the torque error T_{ripple} can be expressed as follows:

$$(T_{\text{ripple}}^2) = \frac{1}{t_{sp}} \int_0^{t_{sp}} (T_{\text{error}})^2 dt = \frac{1}{t_{sp}} \int_{t_s}^{t_{sp}} (T - T^*)^2 dt.$$

It is noted that the study in [10], in each control period t_{sp} , applied a nonzero voltage vector V_k and a zero voltage vector V_0 with time durations t_s and $(t_{sp} - t_s)$, respectively. Therefore, the torque T in these two subintervals could be given as

$$T = \begin{cases} T_{t0} + S_1 t, & 0 \leq t \leq t_s \\ T_{t0} + S_1 t_s + S_0 t - S_0 t_s, & t_s \leq t \leq t_{sp}. \end{cases}$$

Thus, to reduce the torque ripple, the square of the rms torque ripple, defined in the following equation, will be minimized:

$$\begin{aligned} (T_{\text{ripple}}^2)_{\text{old}} &= \frac{1}{t_{sp}} \int_0^{t_s} (S_1 t + T_{t0} - T^*)^2 dt \\ &\quad + \frac{1}{t_{sp}} \int_{t_s}^{t_{sp}} (S_0 t - S_0 t_s + S_1 t_s + T_{t0} - T^*)^2 dt \quad (7) \end{aligned}$$

where T_{t0} and T^* are the initial torque and the torque command, respectively. The optimal time duration t_s spent on the voltage vector V_k satisfies the following equation:

$$\frac{\partial (T_{\text{ripple}}^2)_{\text{old}}}{\partial t_s} = 0. \quad (8)$$

Solving (8), one has

$$t_s = \frac{2T_{\text{error}_t0} - S_0 t_{sp}}{2S_1 - S_0} \quad (9)$$

where $T_{\text{error}_t0} = T_{t0} - T^*$ is the initial torque error. The aforementioned results derived by [10] ensure the minimum rms torque ripple. The concept of the applied voltages and related torque response is shown in Fig. 2.

However, inserting the switching time t_s of (9) into (7), one has the square of the rms torque ripple as

$$(T_{\text{ripple}}^2)_{\text{old}} = \frac{1}{3S_1 t_{sp}} [(S_1 t_s - T_{\text{error_}t0})^3 + T_{\text{error_}t0}^3] + \frac{1}{3S_0 t_{sp}} [(S_0 t_{sp} - S_0 t_s + S_1 t_s - T_{\text{error_}t0})^3 - (S_1 t_s - T_{\text{error_}t0})^3]. \quad (10)$$

Note that the aforementioned minimum square of the rms torque ripple (10) is a function of the initial torque error $T_{\text{error_}t0}$. It means that there exists an optimal value $T_{\text{error_}t0} = T_{\text{error_}t0(\text{opt})}$ which makes the square of the rms torque ripple (10) minimum. To find $T_{\text{error_}t0(\text{opt})}$, one minimizes (7) with respect to $T_{\text{error_}t0}$. Therefore, one has

$$T_{\text{error_}t0(\text{opt})} = \frac{(S_1 - S_0)t_s^2 + S_0 t_{sp}^2 + 2(S_1 - S_0)t_{sp} t_s - 2(S_1 - S_0)(t_{sp} - t_s)t_s}{2t_{sp}}. \quad (11)$$

Substituting (9) and (11) into (7), one obtains the global minimum square rms torque ripple

$$(T_{\text{ripple}}^2)_{\text{opt}} = \frac{t_{sp}^2 S_1^2 S_0^2}{12(S_1 - S_0)^2}. \quad (12)$$

It is noticed that the global minimum rms torque ripple (12) has not been achieved before; in other words, one always has $(T_{\text{ripple}}^2)_{\text{opt}} \leq (T_{\text{ripple}}^2)_{\text{old}}$.

To obtain the global minimum rms torque ripple, this study, in the following, will propose a simple but effective switching method to assure the existence of the global minimum rms torque ripple $(T_{\text{ripple}}^2)_{\text{opt}}$ given by (12).

B. Global Minimum RMS Torque Ripple Strategy

The proposed global minimum rms torque ripple reduction strategy consists of two steps. First, it designs a control to drive the torque error to zero at the following sampling instant. Next, the torque ripple and bias will be effectively reduced by modifying the switching pattern of the applied voltage vectors derived in the last step. The design also applies a nonzero voltage vector and a zero one in a control period based the voltage selection given by Table I. However, this study assures the global minimum rms torque ripple $(T_{\text{ripple}}^2)_{\text{opt}}$ given as (12).

Define the torque relation over a control period t_{sp} as

$$T_{t_{sp}} = T_{t0} + \Delta T_e \quad (13)$$

where $T_{t_{sp}}$ is the electromagnetic torque at the end of a control period. In each control period t_{sp} , a nonzero voltage vector V_k and a zero voltage vector V_0 are applied with time durations t_s and $(t_{sp} - t_s)$, respectively. The torque relation (13) becomes

$$T_{t_{sp}} = T_{t0} + S_1 t_s + S_0 (t_{sp} - t_s). \quad (14)$$

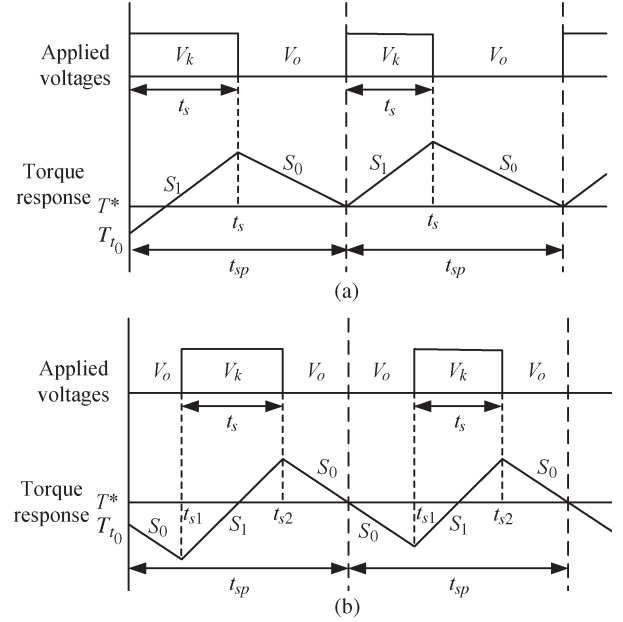


Fig. 3. Applied voltages and torque responses of the proposed global minimum DTC. (a) First-step design. (b) Second-step design.

In addition, let $T_{\text{error_}t0}$ and $T_{\text{error_}t_{sp}}$, respectively, be the torque errors at the beginning and the end of a control period

$$T_{\text{error_}t0} = T_{t0} - T^* \quad (15)$$

$$T_{\text{error_}t_{sp}} = T_{t_{sp}} - T^*. \quad (16)$$

Thus, the torque errors $T_{\text{error_}t0}$ and $T_{\text{error_}t_{sp}}$ could be related by

$$T_{\text{error_}t_{sp}} = T_{\text{error_}t0} + S_1 t_s + S_0 (t_{sp} - t_s). \quad (17)$$

The first step is to determine the time duration t_s , when applying the nonzero voltage vector V_k , to minimize the torque error $T_{\text{error_}t_{sp}}$ at the end of a control period. Thus, it could be done by solving the following equation:

$$\frac{\partial (T_{\text{error_}t_{sp}}^2)}{\partial t_s} = 0. \quad (18)$$

Thus, one obtains

$$t_s = \frac{T_{\text{error_}t0} + S_0 t_{sp}}{S_1 - S_0}. \quad (19)$$

Note that the control will drive the torque error to zero at the end of the control period, if one applies the nonzero voltage vector V_k and zero voltage vector V_0 , respectively, with time durations t_s given by (19) and $(t_{sp} - t_s)$. Once the torque error is driven to zero, the following control cycles could have the zero starting torque error, i.e., $T_{\text{error_}t0} = 0$. Moreover, the zero torque error at the end of the control cycle, $T_{\text{error_}t_{sp}} = 0$, is maintained.

However, directly applying a nonzero voltage vector V_k and a zero voltage vector V_0 with time durations t_s and $(t_{sp} - t_s)$, respectively, will result in a torque bias and large rms ripple. It could be seen in Fig. 3(a). The next step is to reduce the torque bias; at the same time, the control has to reduce the rms torque

ripple. To these ends, the applied voltages will be rearranged in a symmetric manner, as shown in Fig. 3(b). Accordingly, the torque relation (17) becomes

$$\begin{aligned} T_{\text{error}_{t_{sp}}} &= T_{\text{error}_{t_0}} + S_0 t_{s1} + S_1(t_{s2} - t_{s1}) + S_0(t_{sp} - t_{s2}) \\ &= T_{\text{error}_{t_0}} + S_0 \left(\frac{t_{sp} - t_s}{2} \right) + S_1(t_s) + S_0 \left(\frac{t_{sp} - t_s}{2} \right) \end{aligned} \quad (20)$$

where $t_{s1} = (t_{sp} - t_s)/2$ and $t_{s2} = t_{s1} + t_s$ are the switching instants of applied voltage vectors.

It is noted again that the control still drives the torque error to zero even if $T_{\text{error}_{t_0}} \neq 0$. Once the torque error $T_{\text{error}_{t_{sp}}}$ is driven to zero, the following control cycles could have the zero starting torque error, i.e., $T_{\text{error}_{t_0}} = 0$. This means that the starting torque error is controllable, while it is not the cases in [10], [13], and [20].

Thus, the square of the rms torque ripple could be calculated by the following equation:

$$\begin{aligned} (T_{\text{ripple}}^2)_{\text{new}} &= \frac{1}{t_{sp}} \left\{ \int_0^{t_{s1}} S_0^2 t^2 dt + \int_{t_{s1}}^{t_{s2}} [S_0 t_{s1} + S_1(t - t_{s1})]^2 dt \right. \\ &\quad \left. + \int_{t_{s2}}^{t_{sp}} [S_0 t_{s1} + S_1(t_{s2} - t_{s1}) + S_0(t - t_{s2})]^2 dt \right\}. \end{aligned} \quad (21)$$

The square of the rms torque ripple $(T_{\text{ripple}}^2)_{\text{new}}$ could be easily calculated, by inserting t_{s1} and t_{s2} to (21), as

$$(T_{\text{ripple}}^2)_{\text{new}} = \frac{t_{sp}^2 S_1^2 S_0^2}{12(S_1 - S_0)^2}. \quad (22)$$

Observing (22), one is surprised that $(T_{\text{ripple}}^2)_{\text{new}}$ coincides with the global minimum $(T_{\text{ripple}}^2)_{\text{opt}}$ given by (12). Comparing $(T_{\text{ripple}}^2)_{\text{new}}$ with $(T_{\text{ripple}}^2)_{\text{old}}$ and $(T_{\text{ripple}}^2)_{\text{opt}}$, one concludes that

$$(T_{\text{ripple}}^2)_{\text{new}} = (T_{\text{ripple}}^2)_{\text{opt}} \leq (T_{\text{ripple}}^2)_{\text{old}}. \quad (23)$$

The aforementioned result demonstrates that the torque ripple designed by this study has a global minimum rms ripple. Moreover, it is noted that it not only has constant switching frequency but also has no more switching points than [10].

The implementation of the two-step torque ripple reduction algorithm is briefly described as follows.

- 1) The triangular wave is used instead of the sawtooth one for the comparator input when applying the voltage vectors.
- 2) According to Table I, select the needed voltage vector.
- 3) Calculate the ascending and descending torque slopes according to (5) and (6).
- 4) If $T_{\text{error}_{t_0}} \neq 0$, the torque is in the transient condition. If $t_s > t_{sp}$, the selected voltage vector V_k is fully turned on

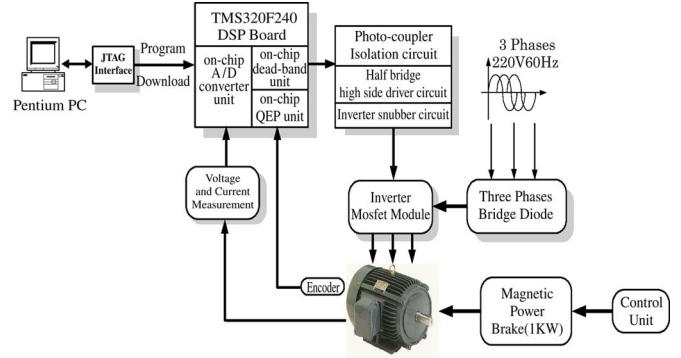


Fig. 4. Experimental setup of the proposed method.

during the whole control period. If $t_s < t_{sp}$, turn on the selected voltage vector V_k for time duration t_s , and then, switch to the zero voltage vector V_0 for the left time of this cycle.

- 5) If $T_{\text{error}_{t_0}} = 0$, the torque is in the steady condition. At the beginning of this cycle, i.e., $t = 0$, keep turning on the zero voltage vector V_0 from the last cycle for time duration t_{s1} . At time $t = t_{s1}$, switch to the selected voltage vector V_k . Keep turning on V_k for time duration t_s until time reaches t_{s2} , and then, switch to the zero voltage vector V_0 until time reaches the end of the control cycle t_{sp} .
- 6) For the next control cycle, return to step 2) and continue.

Remark 1: The derived global minimum rms torque ripple reduction strategy is based on a small control period. Observing the applied voltages shown in Fig. 3(b), one sees that it has two switching times for two different voltage vectors. Thus, for a different switching frequency, the presented method has the global minimum property if the method is subjected to two switching times for two different voltage vectors.

Remark 2: Because the implementation of DTC requires knowing the magnitude and location of the stator flux vector, the information of the stator flux is generally obtained through a pure integrator. It is easily affected by the stator resistance and has the problem of dc drift. To make the presented method more practical, it should be combined with the methods dealing with the problems of the stator resistance tuning and dc drift at low frequencies. Papers dealing with these problems could be found in [27] and [28].

III. SIMULATION AND EXPERIMENTAL RESULTS

To confirm the validity of the proposed DTC method, simulations have been first carried out. Moreover, to make the experimental validation of the effectiveness of the proposed DTC, a DSP-based induction motor drive system has been built as in Fig. 4. The experimental setup consists of the following elements:

- 1) machine unit, a squirrel-cage induction motor, and a magnetic power brake;
- 2) voltage inverter;
- 3) DSP board;
- 4) personal computer (PC).

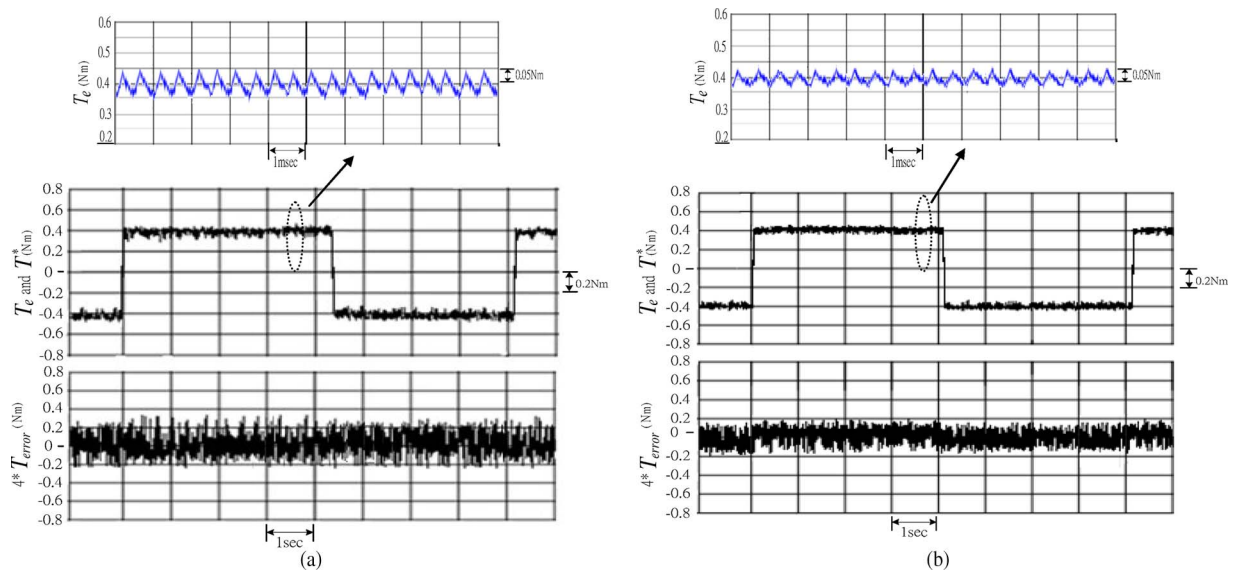


Fig. 5. Simulation torque responses. (a) Minimum ripple DTC [10]. (b) Proposed global minimum DTC.

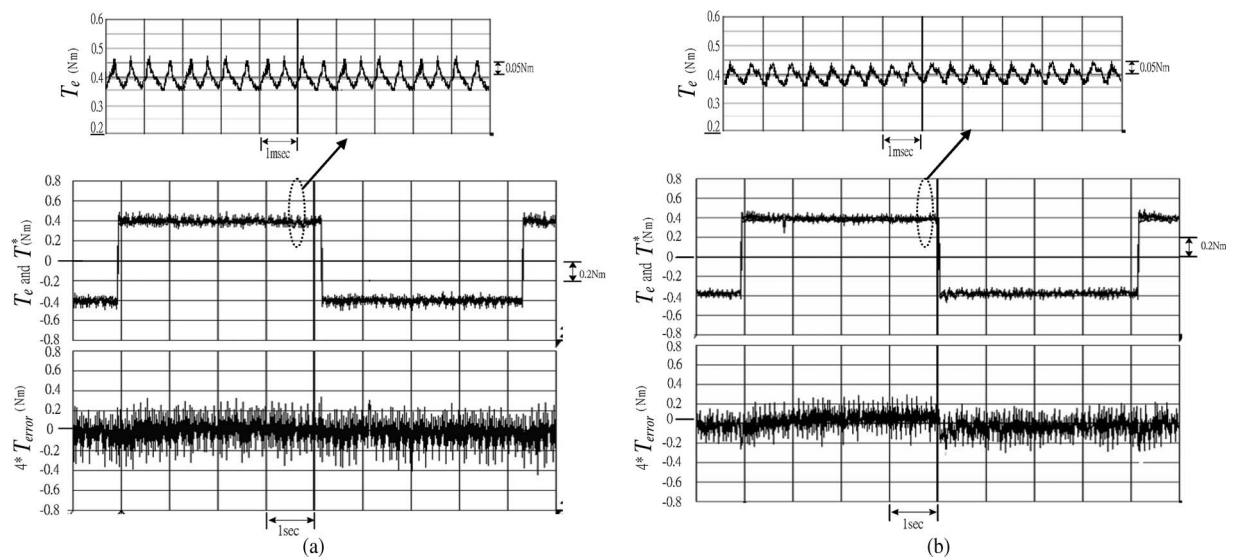


Fig. 6. Experimental torque responses. (a) Minimum ripple DTC [10]. (b) Proposed global minimum DTC.

In the setup, a 0.37-kW, 220-V, 50-Hz, and four-pole induction motor is used. The motor has the following parameters: $R_s = 8.6855 \Omega$, $R_r = 12.3476 \Omega$, $L_s = 679.174 \text{ mH}$, $L_r = 492.814 \text{ mH}$, and $L_m = 463.2639 \text{ mH}$. A magnetic power brake with a control unit provides load to the motor. The motor is fed by a voltage inverter. The inverter is designed using a metal–oxide–semiconductor field-effect transistor module. It is driven by using fast optocouplers. For motor current measurement, two Hall effect transducers are used. The central element of the whole DTC drive system is a control system, TMS320F240 DSP board. It is a 20-MHz fixed-point DSP with on-chip A/D converters. Moreover, a PC is used to download a DTC program to the DSP through a JTAG interface. The sampling time of the DTC experiments is taken as $300 \mu\text{s}$.

Simulations using the MATLAB/Simulink simulation package are first performed when the induction motor, controlled by the proposed DTC, operates at $\pm 0.4 \text{ N} \cdot \text{m}$. For comparison,

the same simulations are carried out under the same operation conditions except that the DTC method proposed in [10] is used instead. Fig. 5(a) and (b) shows, respectively, the torque responses controlled by the proposed DTC and the DTC presented in [10] under the same torque condition $\pm 0.4 \text{ N} \cdot \text{m}$. For more detailed information about the torque ripple, a zoom of the torque response is provided. Next, to verify the feasibility of the built prototype system, experiments are carried out under the same operation conditions as simulations. The related torque responses shown in Fig. 6(a) and (b) are 0.0342 and $0.0308 \text{ N} \cdot \text{m}$, respectively. Thus, both simulation and experimental results verify that the proposed DTC method effectively reduces the torque ripple.

Moreover, except the torque ripple, the relevant phase current and flux responses in Figs. 5 and 6 are shown in Figs. 9 and 10, respectively. Fig. 7(a) and (b) shows the simulated rms current ripples of 0.346 and 0.332 A , respectively, for the method [10]

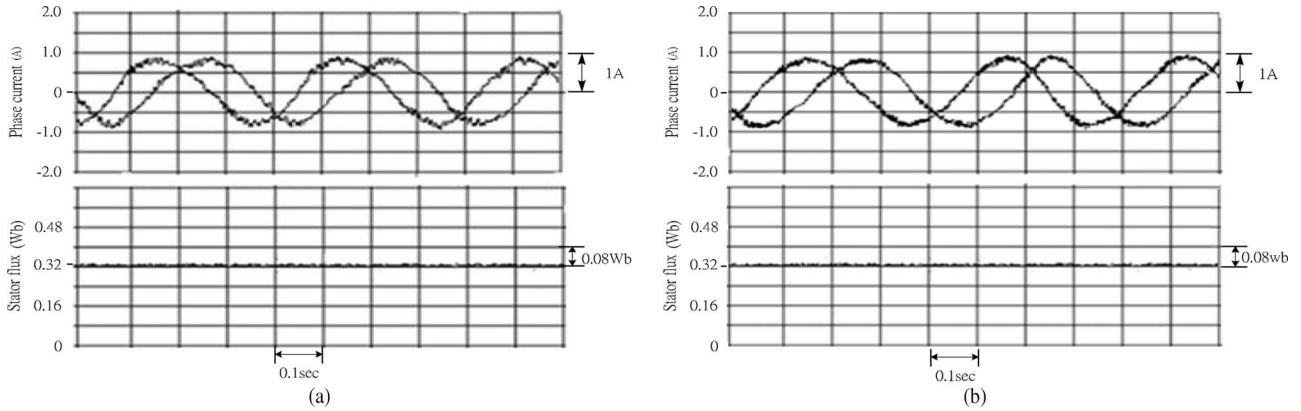


Fig. 7. Simulation stator currents and stator flux under the torque condition $0.4 \text{ N} \cdot \text{m}$. (a) Minimum ripple DTC [10]. (b) Proposed global minimum DTC.

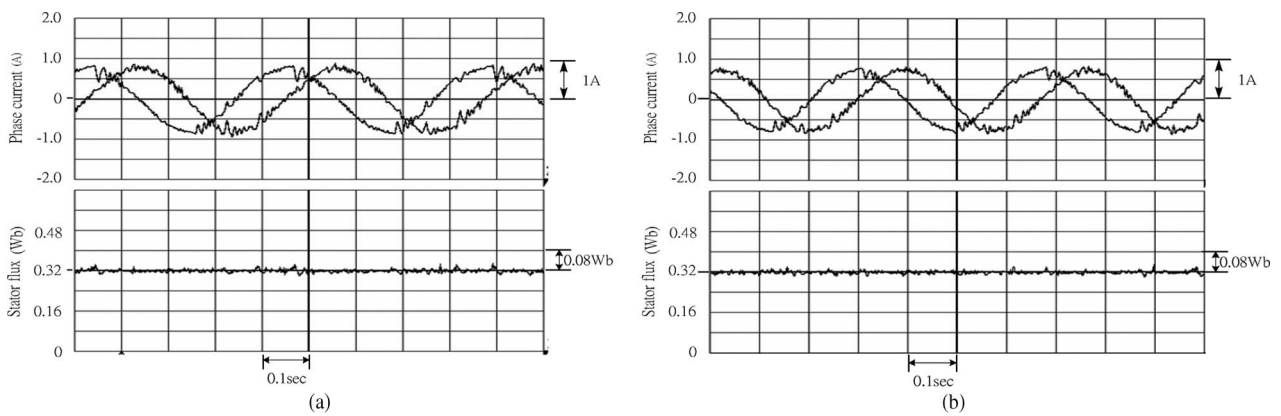


Fig. 8. Experimental stator currents and stator flux under the torque $0.4 \text{ N} \cdot \text{m}$. (a) Minimum ripple DTC [10]. (b) Proposed global minimum DTC.

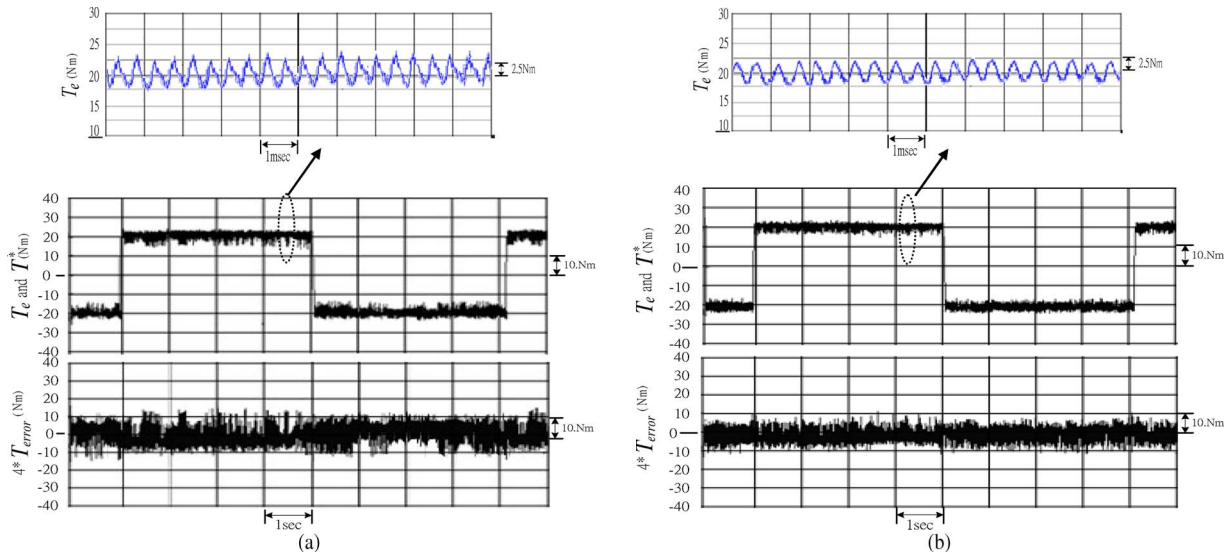


Fig. 9. Simulated torque and torque error responses under the torque of $20 \text{ N} \cdot \text{m}$ ($1 * R_s$ and $1 * R_r$). (a) Minimum ripple DTC [10]. (b) Proposed global minimum DTC.

and the proposed method. Fig. 8(a) and (b) shows the related experimental results and also shows, respectively, the rms current ripples of 0.346 and 0.331 A. Comparing the torque and current responses of the simulated and experimental results shown in Figs. 5–8, one could see that the proposed method has reduced not only the torque ripple but also the current ripple.

Furthermore, to see the effectiveness of the proposed method on a high-power motor, simulations are done for an induction motor (4 kW, 220 V, 50 Hz, and 4 poles). Fig. 9 shows the torque responses of $\pm 20 \text{ N} \cdot \text{m}$. The related rms torque ripples of the DTC method [10] and the proposed method are 1.676 and 1.543 $\text{N} \cdot \text{m}$, respectively. The proposed method is better

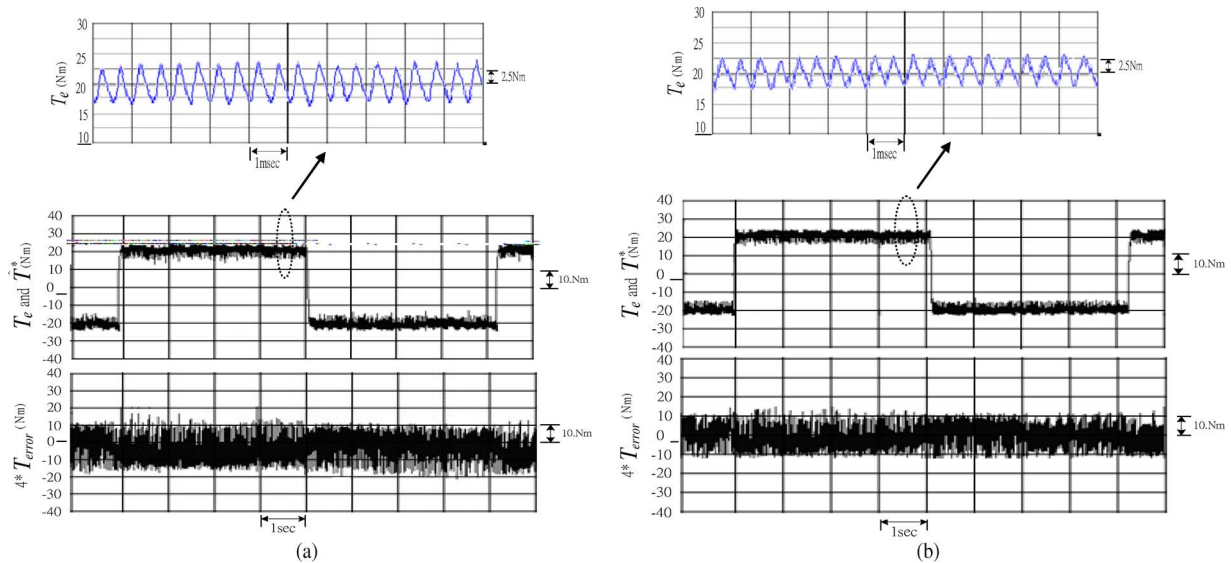


Fig. 10. Simulated torque and torque error responses under the torque of $20 \text{ N} \cdot \text{m}$ ($2^* R_s$ and $2^* R_r$). (a) Minimum ripple DTC [10]. (b) Proposed global minimum DTC.

than the DTC method [10] as expected. Moreover, to see the parameter deviation effect, the same simulation is done by assuming that the stator and rotor resistances are drifted to two times of the nominal values. Fig. 10(a) and (b) shows the related responses as in Fig. 9(a) and (b). The related rms torque ripples are 1.875 and 1.682 $\text{N} \cdot \text{m}$. It can be seen that the performance could be worsened if the stator and rotor resistances are uncertain. This problem is the main problem of the existing method and should be considered by using the parameter adaptation method.

IV. CONCLUSION

This paper has proposed a simple and effective torque ripple minimization method for DTC of induction motor drives. If compared with the previous studies, the proposed method has the advantage of global minimum rms torque ripple.

The feasibility of the study in this paper has also been verified by building a fixed-point TMS320F240 DSP-based induction motor DTC drive system. The simulation and experimental results have demonstrated that the proposed method effectively reduces more rms torque ripples compared with the method of a previous study. Furthermore, the related current ripple is also reduced.

Because the torque ripple is reduced, a possible application will be that the case needs more precise speed control. The main problem left here is the drift of the stator resistance, which results in the stator flux estimation error.

REFERENCES

- [1] E. S. de Santana, E. Bim, and W. C. do Amaral, "Predictive algorithm for controlling speed and motor flux of induction motor," *IEEE Trans. Ind. Electron.*, vol. 55, no. 12, pp. 4398–4407, Dec. 2008.
- [2] K.-K. Shyu and H. J. Shieh, "A new switching surface sliding-mode speed control for induction motor drive systems," *IEEE Trans. Power Electron.*, vol. 11, no. 4, pp. 660–667, Jul. 1996.
- [3] H. J. Shieh and K.-K. Shyu, "Nonlinear sliding-mode torque control with adaptive backstepping approach for induction motor drive," *IEEE Trans. Ind. Electron.*, vol. 46, no. 2, pp. 380–389, Apr. 1999.
- [4] Z. Krzeminski, "Nonlinear control of induction motor," in *Proc. IFAC 10th World Congr. Autom. Control*, Monachium, Germany, 1987, vol. 3, pp. 349–354.
- [5] I. Takahashi and T. Noguchi, "A new quick response and high efficiency control strategy of an induction motor," *IEEE Trans. Ind. Appl.*, vol. IA-22, no. 5, pp. 820–827, Sep./Oct. 1986.
- [6] M. Depenbrock, "Direct self-control (DSC) of inverter-fed induction machine," *IEEE Trans. Power Electron.*, vol. 3, no. 4, pp. 420–429, Oct. 1988.
- [7] T. Habetler, F. Profumo, M. Pastorelli, and L. M. Tolbert, "Direct torque control of an induction machines using space vector modulation," *IEEE Trans. Ind. Appl.*, vol. 28, no. 5, pp. 1045–1053, Sep./Oct. 1992.
- [8] M. P. Kazmierkowski and A. B. Kasprowicz, "Improved direct torque and flux vector control of PWM inverter-fed induction motor drives," *IEEE Trans. Ind. Electron.*, vol. 42, no. 4, pp. 344–350, Aug. 1995.
- [9] S. Mir, M. E. Elbuluk, and D. S. Zinger, "PI and fuzzy estimators for tuning the stator resistance in direct torque control of induction machines," *IEEE Trans. Power Electron.*, vol. 13, no. 2, pp. 279–287, Mar. 1998.
- [10] J. K. Kang and S. K. Sul, "New direct torque control of induction motor for minimum torque ripple and constant switching frequency," *IEEE Trans. Ind. Appl.*, vol. 35, no. 5, pp. 1076–1082, Sep./Oct. 1999.
- [11] D. Casadei, G. Serra, and A. Tani, "Implementation of a direct torque control algorithm for induction motors based on discrete space vector modulation," *IEEE Trans. Power Electron.*, vol. 15, no. 4, pp. 769–777, Jul. 2000.
- [12] C. Lascu, I. Boldea, and F. Blaabjerg, "A modified direct torque control for induction motor sensorless drive," *IEEE Trans. Ind. Appl.*, vol. 36, no. 1, pp. 122–130, Jan./Feb. 2000.
- [13] K. B. Lee and J. H. Song, "Torque ripple reduction in DTC of induction motor driven by three-level inverter with low switching frequency," *IEEE Trans. Power Electron.*, vol. 17, no. 2, pp. 255–264, Mar. 2002.
- [14] C. A. Martins, X. Roboam, T. A. Meynard, and A. S. Carvalho, "Switching frequency imposition and ripple reduction in DTC drives by using a multilevel converter," *IEEE Trans. Power Electron.*, vol. 17, no. 2, pp. 286–297, Mar. 2002.
- [15] D. Casadei, G. Serra, A. Tani, L. Zarri, and F. Profumo, "Performance analysis of a speed-sensorless induction motor drive based on a constant-switching frequency DTC scheme," *IEEE Trans. Ind. Appl.*, vol. 39, no. 2, pp. 476–484, Mar./Apr. 2003.
- [16] N. R. N. Idris and A. H. M. Yatim, "Direct torque control of induction machines with constant switching frequency and reduced torque ripple," *IEEE Trans. Ind. Electron.*, vol. 51, no. 4, pp. 758–767, Aug. 2004.
- [17] A. Tripathi, A. M. Khambadkone, and S. K. Panda, "Torque ripple analysis and dynamic performance of a space vector modulation based control method for AC drives," *IEEE Trans. Power Electron.*, vol. 20, no. 2, pp. 485–492, Mar. 2005.
- [18] K. B. Lee and F. Blaabjerg, "Sensorless DTC-SVM for induction motor driven by a matrix converter using a parameter estimation strategy," *IEEE Trans. Ind. Electron.*, vol. 55, no. 2, pp. 512–521, Feb. 2008.

- [19] X. del Toro Garcia, A. Arias, M. G. Jayne, and P. A. Witting, "Direct torque control of induction motors utilizing three-level voltage source inverters," *IEEE Trans. Ind. Electron.*, vol. 55, no. 2, pp. 956–958, Feb. 2008.
- [20] G. Abad, M. A. Rodriguez, and J. Poza, "Two-level VSC based predictive direct torque control of the double fed induction machine with reduced torque and flux ripples at low constant switching frequency," *IEEE Trans. Power Electron.*, vol. 23, no. 3, pp. 1050–1061, May 2008.
- [21] S. M. A. Cruz, A. Stefani, F. Filippetti, and A. J. M. Cardoso, "A new model-based technique for the diagnosis of rotor faults in RFOC induction motor drives," *IEEE Trans. Ind. Electron.*, vol. 55, no. 12, pp. 4218–4228, Dec. 2008.
- [22] S. Maiti, C. Chakraborty, Y. Hori, and M. C. Ta, "Model reference adaptive controller-based rotor resistance and speed estimation techniques for vector controlled induction motor drive utilizing reactive power," *IEEE Trans. Ind. Electron.*, vol. 55, no. 2, pp. 594–601, Feb. 2008.
- [23] H. Abu-Rub, J. Guzinski, Z. Krzeminski, and H. A. Toliyat, "Advanced control of induction motor based on load angle estimation," *IEEE Trans. Ind. Electron.*, vol. 51, no. 1, pp. 5–14, Feb. 2004.
- [24] M. Wlas, Z. Krzeminski, J. Guzinski, and H. Abu-Rub, "Artificial-neural-network-based sensorless nonlinear control of induction motors," *IEEE Trans. Energy Convers.*, vol. 20, no. 3, pp. 520–528, Sep. 2005.
- [25] M. Wlas, Z. Krzeminski, and H. A. Toliyat, "Neural-network-based parameter estimations of induction motors," *IEEE Trans. Ind. Electron.*, vol. 55, no. 4, pp. 1783–1794, Apr. 2008.
- [26] J. Guzinski, M. Diguët, Z. Krzeminski, A. Lewicki, and H. Abu-Rub, "Application of speed and load torque observers in high-speed train drive for diagnostic purposes," *IEEE Trans. Ind. Electron.*, vol. 56, no. 1, pp. 248–256, Jan. 2009.
- [27] C. Lascu and G. D. Andreescu, "Sliding-mode observer and improved integrator with DC-offset compensation for flux estimation in sensorless-controlled induction motors," *IEEE Trans. Ind. Electron.*, vol. 53, no. 3, pp. 785–794, Jun. 2006.
- [28] G. Buja and R. Menis, "Steady-state performance degradation of a DTC IM drive under parameter and transduction errors," *IEEE Trans. Ind. Electron.*, vol. 55, no. 4, pp. 1749–1760, Apr. 2008.



Kuo-Kai Shyu (M'98) received the B.S. degree in electrical engineering from Tatung Institute of Technology, Taipei, Taiwan, in 1979, and the M.S. and Ph.D. degrees in electrical engineering from National Chung-Kung University, Tainan, Taiwan, in 1984 and 1987, respectively.

Since 1988, he has been with National Central University, Chung-Li, Taiwan, where he is currently a Professor in the Department of Electrical Engineering. From 1988 to 1999, he was a Visiting Scholar in the Electrical and Computer Engineering Department,

Auburn University, Auburn, AL. His teaching and research interests include variable structure control systems and signal processing with applications in motor control, power electronics, and medical instruments.



Juu-Kuh Lin received the M.S. degree in electrical engineering from Tatung Institute of Technology, Taipei, Taiwan, in 1999. He is currently working toward the Ph.D. degree in electrical engineering in the Department of Electrical Engineering, National Central University, Chung-Li, Taiwan.

His research interests include motor control, power electronics, and circuit design.



Van-Truong Pham received the B.S. and M.S. degrees in electrical engineering from Hanoi University of Technology, Hanoi, Vietnam, in 2000 and 2002, respectively. He is currently working toward the Ph.D. degree in the Department of Electrical Engineering, National Central University, Chung-Li, Taiwan.

His research interests include automatic control, medical image processing, and computer vision.



Ming-Ji Yang was born in Yilan, Taiwan, in 1974. He received the B.S. degree in electronic engineering from National Taiwan University of Science and Technology, Taipei, Taiwan, in 1999, and the Ph.D. degree in electrical engineering from National Central University, Chung-Li, Taiwan, in 2009.

He served for two years as an R&D Engineer with Riye Electric Company, Ltd., Taoyuan, Taiwan, (2000–2002). In 2008, he established Inskye Energy Technology Company, Ltd., Taoyuan, where he is currently the General Manager, and the company is developing electric vehicle applications. His research interests include power quality improvement, power electronic control, and electric vehicle design.

Dr. Yang received the Outstanding Research Graduate Student Award from National Central University in 2007.



Te-Wei Wang was born in Keelung, Taiwan, in 1983. He received the B.S. degree in automatic control engineering from Feng Chia University, Taichung, Taiwan, in 2005, and the M.S. degree in electrical engineering from National Central University, Chung-Li, Taiwan, in 2007.

He is currently with the Department of Electrical Engineering, National Central University. His research interests include power electronics, battery chargers, automotive electronics, and A/D mixed signal control circuit design.